Excited-State Double Proton Transfer in 3-Formyl-7-azaindole: Role of the $n\pi^*$ State in Proton-Transfer Dynamics

Pi-Tai Chou,* Guo-Ray Wu, Ching-Yen Wei, Mei-Ying Shiao, and Yun-I Liu

Department of Chemistry, The National Chung-Cheng University, Chia Yi, Taiwan R.O.C.

Received: May 17, 2000; In Final Form: July 25, 2000

3-Formyl-7-azaindole (3FAI) and its derivatives have been synthesized to study the role of the nπ* state in the excited-state double proton transfer (ESDPT) reaction. In 3FAI monomer as well as its associated hydrogen-bonded complexes the lowest excited singlet state has been concluded to be in the ^{1}nπ* configuration. The association constants incorporating the hydrogen bonding formation were determined to be 1.9×10^4 (313 K), 2.2×10^4 (298 K) and 1.8×10^5 M^{-1} (298 K) for 3FAI dimer, 3FAI/azacyclohexanone and 3FAI/acetic acid, respectively, in cyclohexane. In alcohols, the rate of solvent (e.g., methanol) diffusional migration, forming a "correct" precursor for ESDPT, is concluded to be much slower than the rate of $S_{\pi\pi^*} \rightarrow S_{n\pi^*}$ internal conversion which has been deduced to be 4.37×10^{12} s^{-1}. ESDPT is prohibited in the $S_{n\pi^*}$ state of which the relaxation dynamics are dominated by the rate of $S_{n\pi^*} \rightarrow T_{\pi\pi^*}$ intersystem crossing. In contrast, for 3FAI dimer or 3FAI/acetic acid complex possessing intact dual hydrogen bonds the intrinsic ESDPT is competitive with the rate of $S_{\pi\pi^*} \rightarrow S_{n\pi^*}$ internal conversion, resulting in a prominent imine-like tautomer emission. The results provide the first model among 7AI analogues in which the fast rate of $S_{\pi\pi^*} \rightarrow S_{n\pi^*}$ internal conversion serves as an internal clock to examine the mechanism of guest molecules (including the bulk alcohols) assisted ESDPT.

1. Introduction

The dual hydrogen-bonding (HB) dimer of 7-azaindole (7AI) has long been recognized as a simplified model for the HB base pair of DNA,[1−3] which upon electronic excitation undergoes the double proton-transfer reaction, resulting in a large Stokes shifted tautomer emission (e.g., $\lambda_{max} \sim 480$ nm in cyclohexane). At the molecular level, such an excited-state double proton transfer (ESDPT) process provides one possible mechanism for the mutation which has been proposed to be, in part, due to a "misprint" induced by the proton-transfer tautomerism of a specific DNA base pair during replication, recording an error message.[3−5] Recently, much research has focused on the femtosecond dynamics of double proton transfer in the 7AI dimer.[6−10] In the gas phase, the femtosecond TOF-MS result[6] has led to an establishment of a sequential ESDPT mechanism which was further supported by the arrest of a 7AI dimer cationic species via a coulomb explosion technique.[7] On the basis of femtosecond fluorescence upconversion in combination with transient absorption techniques, Fiebig et al.[10] have resolved excitation-wavelength-dependent multiexponential tautomer rise times of the 7AI dimer in nonpolar solvents, which are the basis of a nonconcerted double-proton transfer. Consequently, they concluded that on the global potential energy surface both trajectories of the symmetric and asymmetric vibrational motion coupled with the solvent dynamics must be considered for the proton-transfer reaction. On the other hand, via the formation of a 7AI(host)/guest HB complex the dynamics of ESDPT incorporating guest molecules have also received considerable attention.[11−17] Studies of 7AI complexed to single molecules of carboxylic acids and lactams have revealed rapid ESDPT reaction,[16] especially for the catalytic type of reaction where the guest molecule (e.g., acetic acid) remains unchanged during the reaction. In alcohols and water the dynamics of ESDPT in 7AI and its analogue 7-azatryptophan have been successfully applied to probe the solvation and/or protein dynamics.[11−15] The proton transfer dynamics of 7AI in linear-carbon-chain monoalcohols have been interpreted in terms of a two-step model incorporating solvent rearrangement to a "correct" configuration, followed by a rapid proton transfer which is possibly dominated by a tunneling mechanism. In water solvents the explanations are somewhat scattering in terms of the fraction of correctly solvated 7AI undergoing ESDPT and the relaxation pathways of the tautomer species.[14,15,16a] However, an even slower rate of the solvent reorganization at the first step is generally accepted in water and polyalcohols (vide infra).

More recently, studies have been extended to the dimers of 7AI analogues of biological importance. Among which, purines possessing a similar electronic moiety with respect to 7AI have received particular interest.[18,19] On the basis of a synthetic approach it has been shown that the number as well as the position of the nitrogen atom in either five- or six-member ring system of 7AI alters the relative ESDPT thermodynamics, especially in the noncatalytic type of the proton-transfer reaction. Further focuses on the chemical modification of 7AI are of particular interest to study the substituent effect on the proton-transfer reaction. In this paper we report the spectroscopic and dynamic studies of 3-formyl-7-azaindole (3FAI, see Figure 1) of which the lowest excited singlet state is concluded to be in the ^{1}nπ* configuration in its monomer as well as in HB complexes. Consequently, the fast rate of $S_{\pi\pi^*} \rightarrow S_{n\pi^*}$ internal conversion (IC) serves as an internal clock to examine the mechanism of guest molecules coupled ESDPT reaction.

2. Experimental Section

2.1. Materials. 7-Azagramine ($C_{10}H_{13}N_3$), a precursor for synthesizing 3-formyl-7-azaindole, was synthesized according

10.1021/jp001807g CCC: $19.00
Published on Web 09/13/2000

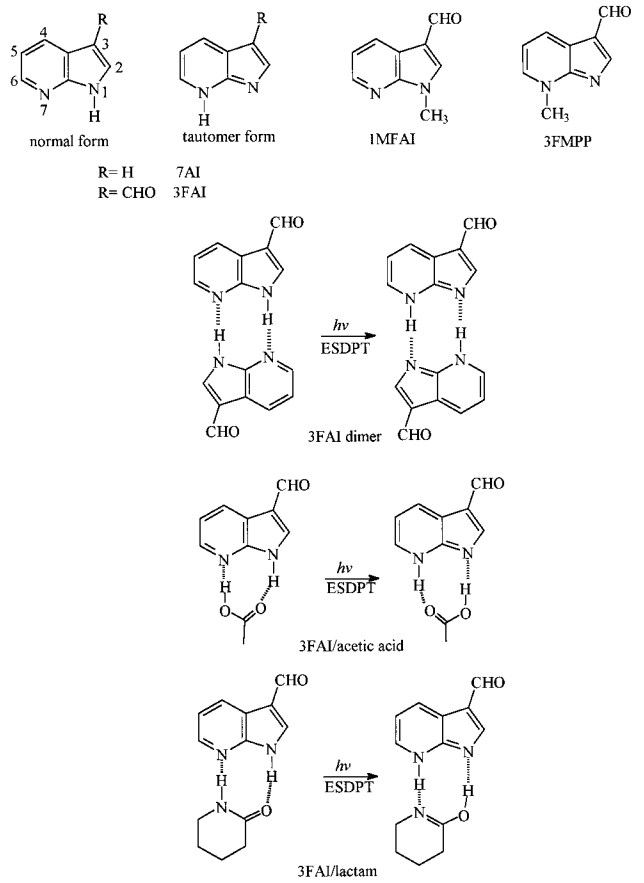

Figure 1. Structures of 7AI, 3FAI and the corresponding derivatives and HB complexes.

to Robison and Robison.[20] The crude product was purified by column chromatography using ethyl acetate as an eluent to obtain 7-azagramine. NMR analyses: ^{1}H NMR (400 MHz, $CDCl_3$) δ 2.266 (s, 6H), 3.608 (s, 2H, CH_2), 7.079 (m, 1H), 7.256 (s, 1H), 8.037 (d, J = 6.32 Hz, 1H), 8.306 (d, J = 3.2 Hz, 1H), 10.22 (b, 1H).

3FAI was prepared through the hydrolysis of 7-azagramine.[20] The crude product was purified by recrystallization from water followed by column chromatography using ethyl acetate as an eluent. ^{1}H NMR (300 M Hz, $CDCl_3$) δ 7.31 (m, 1H), 8.02 (s, 1H), 8.45 (m, 1H), 8.65 (m, 1H), 10.05 (s, 1H, CHO), 10.89 (b, 1H, NH).

1-Methyl-3-formyl-7-azaindole (1MFAI) was synthesized by adding sodium hydride (57%, 60 mg) to the THF solution containing 3FAI (0.15 g), followed by the addition of methyl iodide (30 mg). ^{1}H NMR ($CDCl_3$, 200 MHz): δ 3.99 (s, 3H), 7.22 (t, J = 3.2 Hz, 1H), 7.82 (s, 1H), 8.40 (d, J = 3.2 Hz, 1H), 8.52 (d, J = 6.4 Hz, 1H), 9.92 (s, 1H).

3-Formyl-7-methyl-7*H*-pyrrolo[2,3-*b*]pyridine (3FMPP, see Figure 1) was synthesized by the reaction of 3FAI (0.15 g) and CH_3I (0.70 g) in THF under N_2. NaOH (2.5 N, 10 mL) was then added and the mixture was stirred for ~20 min to obtain 3FMPP (60 mg). ^{1}H NMR ($CDCl_3$, 200 MHz): δ 4.44 (s, 3H), 7.22 (t, J = 8.0 Hz, 1H), 7.83 (d, J = 6.4 Hz, 1H), 8.44 (s, 1H), 8.87 (d, J = 7.8 Hz, 1H), 10.03 (s, 1H).

Cyclohexane and various alcohols are of spectrograde quality (Merck Inc.) and used right after received. Acetic acid (Merck Inc.) was purified through a fractional distillation. Azacyclohexanone (Aldrich) was recrystallized twice from methanol. Since the stable conformer of 2-azacyclohexanone is in the lactam form we thus use the abbreviation "lactam" in order to distinguish it from the "lactim" form (see Figure 1). The N(1) deuterated 3FAI (3FAI(D)) and lactam (lactam (D)) was synthesized by dissolving 3FAI (or lactam) in CH_3OD. CH_3OD was then gradually evaporated in the vacuum line. This procedure was repeated three times and the product was stored in the N_2 purged drybox where the sample preparation was also performed. The formation of 3FAI(D) and lactam(D) was checked by proton NMR where ~92% and 90% of the N−H proton for 3FAI and lactam, respectively disappeared after deuteration. The deuterated acetic acid (CH_3COOD, 98%, Arcose) was purchased from Aldrich and used without further purification.

2.2. Measurements. Steady-state absorption and emission spectra were recorded by a Varian (Cary 3E) spectrophotometer and a Hitachi (F4500) fluorimeter, respectively. Both wavelength-dependent excitation and emission response of the fluorimeter have been calibrated according to a previously reported method.[16] Room-temperature fluorescence quantum yields were measured using quinine sulfate/1.0 N H_2SO_4 as reference, assuming a yield of 0.564 with 365 nm excitation.[21] For the phosphorescence measurement an Nd:YAG (fourth harmonic, 266 nm) was used as a excitation source. The emission was collected at a right angle with respect to the excitation source and detected by an intensified charge coupled detector (ICCD, Princeton Instrument, model 576G/1). Typically, 100 laser shots were collected and averaged in each data acquisition period. Naphthalene was used as a standard to measure the relatively phosphorescence yield, of which the phosphorescence yield was known to be 0.1 in a 77 K EPA (v/v 2:2:5, ether−isopentane−ethyl alcohol) glass.[22]

Nanosecond lifetime measurements have been previously described.[16d] Picosecond lifetime measurements were achieved by using either second (380−420 nm) or third (260−275 nm) harmonic of the femtosecond Ti−Sapphire oscillator (82 MHz, Spectra Physics) as an excitation source. An Edinburgh OB 900-L time-correlated single photon counter was used as a detecting system. Since the fwhm of the excitation pulse is typically ~120 fs, the resolution is limited by the detector response of ~30 ps. The fluorescence decays were analyzed by the sum of exponential functions with an iterative convolution method reported previously.[21] This procedure should allow partial removal of the instrument time broadening and consequently renders a temporal resolution of ~15 ps.

The nanosecond pump−probe transient absorption experiment was performed by using a modified flash lamp (EG&G model LS-1130, ~50 ns pulse width) as a white-light probe pulse. A cylindrical lens was used to shape the pump Nd:YAG 355 nm (~8 ns, Continuum Surlite II) pulse to a rectangular size of 40 × 2 mm^2. The white-light probe pulse was then collected by an optical fiber, collimated by a 5 cm focal length lens, and skimmed by a slit to obtain a 2 × 2 mm^2 rectangular shape before entering the sample cell. Both pump and probe pulses were crossed by a 90° angle with an overlapping distance of 4 cm. The probe white light pulse, after passing through the sample solution, was focused on the entrance of the slit (300 μm) of the ICCD system. With an average of 100 shots an absorbance as low as 10^{-3} can be detected in the spectral range of 300−700 nm.

Details of the theoretical approach (6-31G(d,p)) for the thermodynamics of 3FAI HB complexes in the ground state has been previously described.[23] The calculation of the lower lying excited singlet states was performed by either Cis (singlet, Nstats = 6)[24] or Td (singlet, Nstats = 6)[25−27] method incorporating B3LYP/6-311++G(2d,p) basis sets. However, both methods give negligible differences regarding the lowest energy level of the singlet excited state in 3FAI.

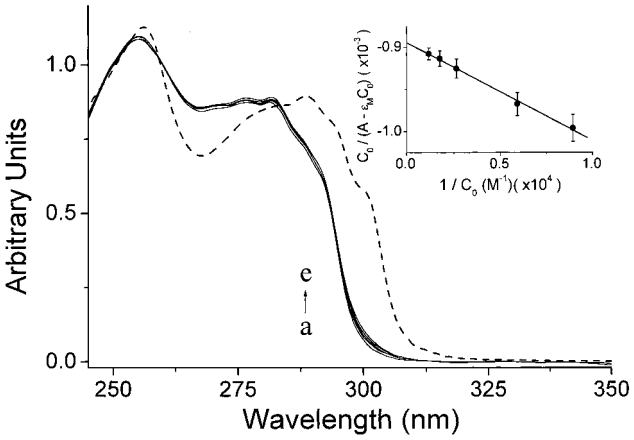

Figure 2. (—) Concentration-dependent absorption spectra of 3FAI in cyclohexane, in which 3FAI (C_0) was prepared at (a) 2.8×10^{-5}, (b) 5.6×10^{-5}, (c) 1.7×10^{-4}, (d) 3.8×10^{-4}, and (e) 8.6×10^{-4} M. The absorption spectra are normalized at 260 nm. (- - -) Absorption spectrum of 1MFAI (1.0×10^{-5} M) in cyclohexane. Inset: Plot of $C_0/(A^{300} - \epsilon_M^{300} C_0)$ values versus $1/C_0$ for a−e and a best nonlinear least-squares fitting curve using eq 1.

The following sections are organized according to a sequence of steps where we first performed detailed absorption and fluorescence titration experiments to determine the thermodynamic and ESDPT properties of 3FAI HB complexes. The results in combination with triplet−triplet transient absorption measurement and low-temperature phosphorescence experiments lead us to deduce the competitive rate of $S_{n\pi^*} \rightarrow S_{\pi\pi^*}$ IC versus the rate of proton-transfer reaction. On the basis of this proposed IC/ESDPT mechanism proton-transfer tautomerism mediated by various types of the guest molecule was discussed in details.

3. Results

3.1. HB Association. When the concentration was prepared to be as low as 8.0×10^{-6} M, 3FAI exhibits the first $\pi \rightarrow \pi^*$ absorption band maximum at 282 nm ($\epsilon_{282} \sim 6214$ M^{-1} cm^{-1}). The spectral feature is similar to that of 1-methyl-3-formyl-7-azaindole (1MFAI) that is generally treated as a nonproton-transfer model due to the lack of an N−H proton. Thus, the assignment of the 282 nm band to the amine-like monomer species is unambiguous. Upon increasing the concentration, changes in the spectral features were observed in which a red shift of the spectra appears in the spectral range of >280 nm (see Figure 2a−e). Note that due to the sparse solubility in nonpolar solvents the titration experiment was performed in cyclohexane at 313 K (40 °C). In comparison, 1MFAI revealed an unchanged absorption profile in the same range of concentrations as 3FAI. The results suggest the formation of 3FAI dimer and/or higher-order aggregates through a hydrogen bonding effect. Similar to that proposed in 7AI,[16] we assume that the geometrical structure of the 3FAI dimer possesses a cyclic dual hydrogen bonding configuration (see Figure 1) where the dual HB sites, i.e., pyrrolic proton (N(1)H) and the pyridinal nitrogen (N(7)) in 3FAI, act as a proton donor and acceptor, respectively. Consequently, a competitive equilibrium between the monomer and its self-associated dimer incorporating dual hydrogen bonds can be established. When the experimental condition was manipulated so that the fraction of 3FAI dimer formation is less than 15%, the absorbance of the mixture at a given wavelength as a function of initially prepared C_0 can be expressed by[19]

$$\frac{C_0}{A - \epsilon_M C_0} = \frac{1}{K_a(\epsilon_D - 2\epsilon_M)}\frac{1}{C_0} + \frac{4}{\epsilon_D - 2\epsilon_M} \qquad (1)$$

In eq 1 ϵ_M and ϵ_D are molar extinction coefficients of the monomer and dimer monitored at a specific wavelength, e.g., 300 nm, where an appreciable percentage of absorbance can be attributed to the self-associated species. Under a sufficiently low 3FAI concentration where only monomer exists, ϵ_M^{300} was calculated to be ~930 M^{-1} cm^{-1}. A plot of $C_0/(A - \epsilon_M C_0)$ at 300 nm as a function of $1/C_0$ shown in the inset of Figure 2 reveals a sufficiently linear behavior, supporting the assumption of dimeric formation in 3FAI. Accordingly, by fixing the ϵ_M value, a linear least-squares fit using eq 1 gives a K_a values to be 1.9×10^4 M^{-1} (313 K) in cyclohexane.

Figure 3 shows the absorption spectra of 3FAI upon adding the acetic acid in cyclohexane. In this experiment, the initial concentration of 3FAI, C_0, was prepared to be as low as 9.5×10^{-6} M to avoid the self-dimerization. The formation of 3FAI/acetic acid HB complexes can be clearly shown by the growth of an absorption band at ~297 nm accompanied by an appearance of isosbestic point at ca. 285 nm throughout the titration, indicating the existence of equilibrium with a common intermediate. On the basis of the assumption of 3FAI complexed by stoichiometrically equivalent guest molecules (e.g., acetic acid), the relationship between the measured absorbance as a function of the initially prepared acetic acid concentration, C_g, can be expressed by[19]

$$\frac{A_0}{A - A_0} = \left(\frac{\epsilon_M}{\epsilon_C - \epsilon_M}\right)\left[\frac{1}{K_a C_g} + 1\right] \qquad (2)$$

where ϵ_M and ϵ_C are molar extinction coefficients of the 3FAI monomer and HB complex, respectively at a specific wavelength. The straight-line plot of $A_0/(A - A_0)$ as a function of $1/C_g$ at a selected wavelength of 300 nm (see inset of Figure 3) supports the validity of the assumption of a 1:1 3FAI/acetic acid complex formation. Consequently, a best linear least-squares fit using eq 2 deduces ϵ_M^{300} and K_a to be 2742 M^{-1} cm^{-1} and 1.8×10^5 M^{-1}, respectively. Remarkable 1:1 3FAI/lactam HB association was also observed in the absorption titration study, and a K_a value was determined to be 2.2×10^4 M^{-1} (298 K, see Table 1). In comparison, although 1MFAI provides one hydrogen-bonding site (i.e., the pyridinal nitrogen) negligible spectral change was observed upon adding either acetic acid or lactam with concentrations up to 10^{-3} M. The result unambiguously supports the formation of cyclic dual hydrogen bonds in both 1:1 3FAI/acetic acid and 3FAI/lactam complexes.

3.2. Emission Properties of the 3FAI. Table 1 lists the steady-state emission properties as well as relaxation dynamics for 3FAI and its HB species in cyclohexane. In contrast to the prominent normal monomer emission in the case of 7AI ($\lambda_{max} \sim 320$ nm with $\Phi_f \sim 0.22$ in cyclohexane[13,14]), an attempt to detect the fluorescence associated with 3FAI monomer (<1.0×10^{-5} M in cyclohexane) in the spectral range of <350 nm failed. Similar nonluminescence behavior was observed for 1FMAI in room temperature cyclohexane. Upon increasing the 3FAI concentration, a unique long-wavelength emission maximum at 437 nm gradually appears (see Figure 4). At an initially prepared concentration C_0 of < 10^{-3} M where the dimer concentration is significantly lower than that of the monomer, a plot of the inverse of 437 nm emission intensity versus $1/C_0^2$ reveals a straight line behavior. The results suggest the precursor of the 437 nm band to be the 3FAI dimer. Further supporting

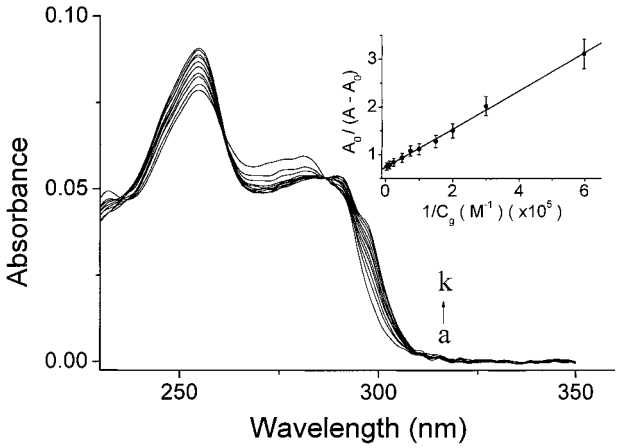

Figure 3. Concentration-dependent absorption spectra of 3FAI (9.4×10^{-6} M) in cyclohexane by adding various acetic acid concentrations (C_g) of (a) 0, (b) 1.7×10^{-6}, (c) 3.3×10^{-6}, (d) 5.0×10^{-6}, (e) 6.7×10^{-6}, (f) 1.0×10^{-5}, (g) 1.5×10^{-5}, (h) 2.0×10^{-5}, (i) 4.0×10^{-5}, (j) 7.6×10^{-5}, and (k) 2.0×10^{-4} M. Inset: Plot of $A_0/(A - A_0)$ at 300 nm as a function of $1/C_g$ in curves b−k and a best least-squares fitting curve using eq 2.

evidence can be given by the excitation maximum of 290 nm which is ~8 nm red shifted with respect to that of the absorption spectrum mainly attributed to the monomer (see Figure 4). Consequently, the 437 nm emission band with a Stokes shift of $\sim 10^4$ cm^{-1} (peak-to-peak) leads us to conclude the occurrence of ESDPT in the 3FAI dimer, resulting in a tautomer emission. This viewpoint can be further supported by the observation of a 458 nm emission ($\tau_f \sim 12.3$ ns) for 3FMPP in cyclohexane (Figure 4). Note that 3FMPP generally serves as a model of the 3FAI tautomeric form (see Figure 1). The dimeric tautomer emission shows an unresolved rise time followed by a single-exponential decay rate of 1.3×10^8 s^{-1} ($\tau_f \sim 7.7$ ns), indicating that the rate of ESDPT for the 3FAI dimer should be >15 ps^{-1} of our system response time (see the Experimental Section).

Figure 5 shows the fluorescence spectra of 3FAI as a function of acetic acid concentrations in cyclohexane. Upon excitation in the region of the isosbestic point of ~285 nm where both 3FAI and 3FAI/acetic acid complex absorb, an enormously large Stokes shifted fluorescence was observed maximum at ~445 nm. The dynamics of relaxation of this 445 nm emission band were found to be excitation-wavelength independent and revealed a single-exponential decay rate of 8.9×10^7 s^{-1} ($\tau_f \sim 11.2$ ns) in the spectral region of 400−550 nm. The large Stokes shift of $>10\,000$ cm^{-1} leads to the assignment of the 445 nm band to the tautomer emission unambiguously. Furthermore, a careful lifetime analysis shows an unresolved rise of the tautomer emission under a system response time of ~15 ps. Similarly, a unique tautomer fluorescence (440 nm, $\tau_f \sim 7.8$ ns) was also observed upon exciting the 3FAI/lactam dual HB complex (see Table 1). However, the observed fluorescence yield is only ~6.7% of the 3FAI/acetic acid complex. Note that for the three studied HB complexes normal emission was not detected in the spectral range of 300−400 nm. Detailed discussion regarding mechanism of IC/ESDPT competing dynamics will be presented in the later section.

Because of the lack of normal fluorescence for both 3FAI monomer and its associated HB complexes, the tautomer emission in 3FAI/acetic acid and 3FA/lactam HB complexes is well resolved. Hence, the association constant can be obtained more precisely from the fluorescence titration studies based on the relation depicted in eq 3

$$\frac{1}{F_p} = (2.3\alpha I_0 \epsilon_c \phi_{obs} C_0)^{-1}\left(1 + \frac{1}{K_a}\frac{1}{C_g}\right) \qquad (3)$$

where C_g represents the added acetic acid (or lactam) concentration, F_p denotes the integrated fluorescence intensity, Φ_{obs} is the measured tautomer fluorescence quantum yield, I_0 and α denote the instrument factor (such as sensitivity, alignment, etc.) and the excitation source intensity, respectively. During the titration experiment where the detection geometry, excitation intensity and the initially prepared 3FAI concentration remain unchanged, the plot of $1/F_p$ versus $1/C_g$ shown in the inset of Figure 5 exhibits good linear behavior, reconfirming the formation of a 1:1 3FAI/acetic acid dual HB complex. A best linear least-squares fit gives the slope and intercept to be 3.1×10^{-7} and 0.034, respectively. Consequently, a K_a value of 1.1×10^5 M^{-1} was obtained. On the basis of the same approach a K_a value was deduced to be 2.8×10^4 M^{-1} for the 3FAI/lactam complex. Both results, within experimental error, are consistent with that obtained from the absorption titration study.

Deuterium isotope effect in the steady-state emission intensity was observed among the three studied 3FAI/guest HB complexes. The tautomer emission intensity of 3FAI(D) dimer, 3FAI(D)/acetic acid(D) and 3FAI(D)/lactam(D) was found to be 0.64, 0.71, and 0.40 relative to their corresponding nondeuterated HB complexes. Note that such a significant isotope-dependent tautomer emission intensity was not observed in the cases of three corresponding 7AI HB complexes in cyclohexane. Details will be elaborated in the discussion section.

In alcohols differences between 3FAI and 7AI are even more remarkable. In methanol 3FAI exhibits an extremely weak tautomer emission maximized at 460 nm. By integrating the emission intensity and comparing with that of the 7AI tautomer in methanol of which Φ_{obs} was known to be 2.4×10^{-3},[14b] one obtained an Φ_{obs} value of 9.5×10^{-5} (see Table 1). Extremely weak tautomer emission was also observed in other linear-chain alcohols such as ethanol and propanol. For all alcohols studied no emission band ascribed to the normal emission was detectable in the spectral region of 300−400 nm. In *tert*-butyl alcohol and polyalcohols such as ethylene glycol the tautomer emission was too weak to be detected. When the fluorimeter was operated under the same amplification and optical configuration throughout the study the sensitivity limit defined as the signal/noise ratio to be <3 was estimated to be $\sim 3.0 \times 10^{-5}$. We thus concluded that the yield of tautomer fluorescence of 3FAI in *tert*-butyl alcohol, if there is any, should be as low as 3.0×10^{-5}. In comparison, prominent dual emission consisting of normal and tautomer fluorescence was observed for 7AI in linear long-chain monoalcohols as well as polyalcohols.[1−3,11−15]

4. Discussion

4.1. Relaxation Pathways in 3FAI. The nonluminescent behavior of 3FAI in the monomeric form is intriguing. In comparison, a high quantum yield ($\Phi_f \sim 0.22$) of the monomer emission has been reported for 7AI in cyclohexane.[13,14] For the case of 7AI monomer, there exist two close low-lying excited singlet states possessing the $\pi\pi^*$ character, which are generally assigned to ^1L_a and ^1L_b states. This assignment is analogous to those defined in the linear condensed polyacenes[28] and indoles[29] where L_a and L_b states are different in the nodal distributions of their wave functions, resulting in a difference in the dipole moment. A semiempirical approach suggests the ^1L_b state to be the lowest excited singlet state in 7AI, while the ^1L_a state is

TABLE 1: Thermodynamic and Photophysical Properties of 3FAI and 3FAI HB Complexes and Its Methylated Derivatives in Cyclohexane

	absorption $\lambda_{max\ (nm)}$	florescence $\lambda_{max\ (nm)}$	Φ_{obs}	τ_f (ns)	K_a (M^{-1}) (298 K)
3FAI	282, 255	NA	NA	NA	
	286, 260[g]	460	9.5×10^{-5}	~8.3[b]	
3FAI dimer	290[a]	437	0.021	7.7	1.9×10^{4} [d]
3FAI(D) dimer	239[a]	437	0.013	7.8	
3FAI/ACID[c]	292[a]	445	0.042	11.2	1.8×10^{5}
3FAI(D)/ACID(D)	292[a]	445	0.030	11.3	1.1×10^{5} [e]
3FAI/LACTAM	292[a]	440	0.0028	7.8	2.2×10^{4}
3FAI(D)/LACTAM(D)	292[a]	440	0.0011	7.8	2.8×10^{4} [e]
1MFAI	290	NA	NA	NA	
3FMPP	375, 425[f]	458	0.085	12.3	
			0.07[g]	11.3[g]	

[a] Values were obtained from the fluorescence excitation spectrum. [b] This value is subject to a larger uncertainty due to the extremely weak emission intensity. [c] ACID denotes acetic acid. [d] Values were obtained at 313 K. [e] Data were obtained from the fluorescence titration experiment. [f] The first vibronic peak of the S_0-S_1 ($\pi\pi^*$) transition. [g] Data were obtained in methanol. NA: not available.

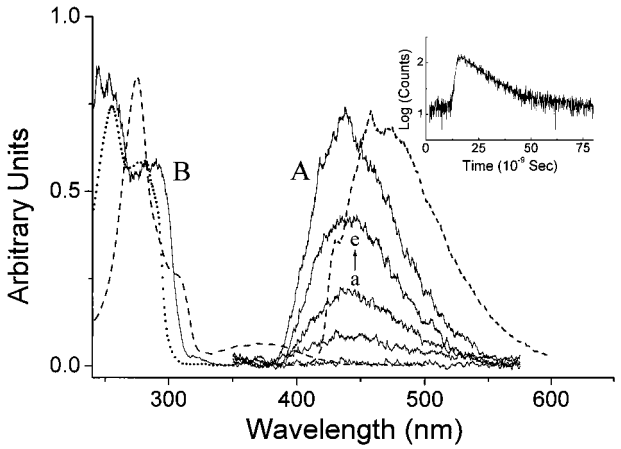

Figure 4. (—) A. Concentration-dependent fluorescence spectra of 3FAI in cyclohexane, in which 3FAI was prepared at (a) 7.1×10^{-6}, (b) 5.6×10^{-5}, (c) 2.5×10^{-4}, (d) 5.7×10^{-4}, and (e) 8.6×10^{-4} M. B. Excitation spectrum of sample c. monitored at 440 nm. (···) The absorption spectrum of sample c. (- - -) Absorption and fluorescence spectra of 3FMPP in cyclohexane (1.5×10^{-5} M). Inset: Time-dependent fluorescence of 3FAI (1.0×10^{-3} M) monitored at 450 nm (λ_{ex}: 300 nm) fitted by one single-exponential decay ($\tau = 7.7$ ns, $\chi^2 = 1.005$).

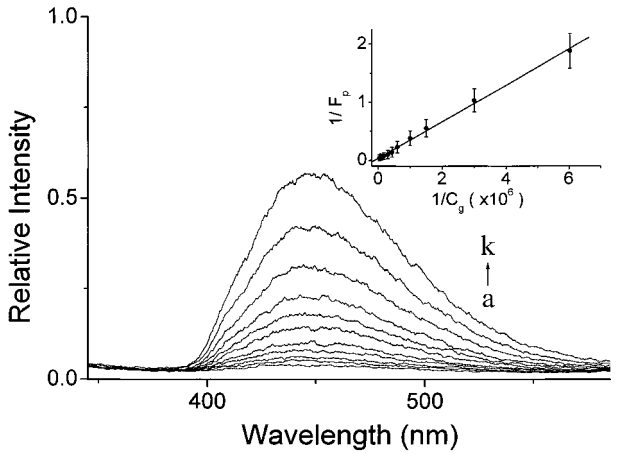

Figure 5. Fluorescence spectra as a function of the acetic acid concentration (C_g) which was prepared to be (a) 0, (b) 1.7×10^{-7}, (c) 3.3×10^{-7}, (d) 6.7×10^{-7}, (e) 1.0×10^{-6}, (f) 1.7×10^{-6}, (g) 2.3×10^{-6}, (h) 3.3×10^{-6}, (i) 5.6×10^{-6}, (j) 1.1×10^{-5}, and (k) 2.5×10^{-5}. Inset: Plot of $1/F_p$ of the integrated 450 nm emission band as a function of $1/C_g$ in curves b−k and a best least-squares fitting curve using eq 3.

higher in energy by ~2000 cm^{-1} in the gas phase.[30] In the solution phase, due to the solvation effect these two excited sates are believed to be located even more closely since the ^1L_b and ^1L_b bands are essentially unresolved on the basis of a steady-state fluorescence excitation anisotropy experiment.[15f] The carbonyl substitution at the C(3) position of 7AI, forming 3FAI, does not likely change the location of L_a and L_b state significantly, as indicated by the similar absorption spectrum in the region of 270−300 nm between 7AI and 3FAI. However, a salient absorption feature maximized at ca. 255 nm for 3FAI is absent in the case of 7AI monomer (see Figure 2). In light of the structural difference between 7AI and 3FAI being the formyl functional group at the C(3) position the 255 nm absorption band is then tentatively assigned to be a highly excited $S_0 \rightarrow S_n$ ($n > 1$, $\pi\pi^*$) transition in 3FAI incorporating the carbonyl π electron. Accordingly, the carbonyl oxygen should also introduce an $n \rightarrow \pi^*$ transition which is plausibly in the lowest excited singlet state. This proposal can be qualitatively supported by an ab initio approach based on the B3LYP/6-311++G(2d,p) basis sets (see the Experimental Section) which estimates the lowest singlet excited state to be a forbidden transition (oscillator strength $f \sim 0$) located at ~327 nm in the gas phase. In contrast, the allowed L_b band was calculated to be the lowest singlet excited state in 7AI.[31] Upon a Franck−Condon excitation, the $\pi\pi^*$ state should carry oscillator strength much higher than that of the $n\pi^*$ level. Consequently, a fast $^1\pi\pi^* \rightarrow {}^1n\pi^*$ IC should take place prior to the ^1L_b (or ^1L_a) $\rightarrow S_0$ relaxation, resulting in a ~unity population in the $S_{n\pi^*}$ state. Owing to the orbital forbidden $S_{n\pi^*} \rightarrow S_0$ transition the deactivation of the $S_{n\pi^*}$ state is expected to be dominated by intersystem crossing (ISC). Thus, an appreciable population in the triplet state is expected, of which the relaxation dynamics are commonly dominated by radiationless pathways in solution phase at ambient temperature. Such a consequence rationalizes the nonluminescence behavior of 3FAI.

To verify this proposed relaxation mechanism, several attempts focusing on identifying the triplet state were carried out. In a 77 K methylcyclohexane glass, 3FAI exhibits a phosphorescence maximum at 525 nm (Figure 6) of which the emission yield (Φ_p) and lifetime (τ_p) were measured to be ca. 10^{-3} and 1.5 μs, respectively. We also carried out a nanosecond transient absorption measurement. Inset of Figure 6 reveals the transient absorption spectrum of 3FAI in degassed cyclohexane upon 266 nm excitation. The decay of the transient absorption, within experimental error, follows single exponential kinetics with a lifetime of ca. 800 ns. The rise time is too fast to be resolved by our current transient absorption system of ca. 30 ns. The decay dynamics are strongly quenched by the addition of O_2 with a quenching rate of ~2.2×10^9 M^{-1} s^{-1} which is

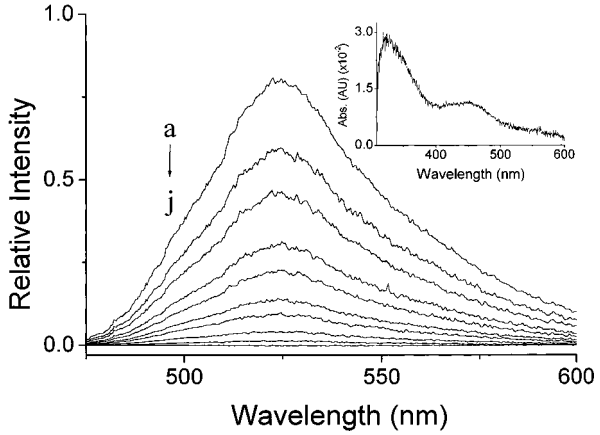

Figure 6. Time-dependent spectral evolution of the phosphorescence of 3FAI in a 77 k methylcyclohexane glass ($\lambda_{ex} \sim 266$ nm) at (a) 320 ns, (b) 350 ns, (c) 450 ns, (d) 550 ns, (e) 650 ns, (f) 1 μs, (g) 1.5 μs, (h) 2.5 μs, (i) 4.5 μs, and (j) 10 μs. Note that an extremely low concentration of 1.0×10^{-7} M was used in this study to minimize the low-temperature aggregation of 3FAI. Inset: the transient absorption spectrum of 3FAI (1.0×10^{-5} M, $\lambda_{ex} \sim 266$ nm) in the degassed cyclohexane. The spectrum was obtained at a pump−probe delay time of 200 ns.

approximately one-ninth of the diffusion-controlled rate in cyclohexane. Since the triplet state with its energy of >8000 cm^{-1} is commonly deactivated by O_2 through an energy transfer mechanism, i.e., $T_1 + {}^3O_2 \rightarrow S_0 + {}^1O_2$, the observed transient absorption with nearly diffusion-controlled O_2 quenching rate can be reasonably ascribed to the triplet−triplet transition.[32] On the basis of the electronic configuration and the group-theoretical argument in combination with numerous experimental results, El-Sayed[34] concluded that the rate of ISC should qualitatively be 3 orders of magnitude larger between states with different configuration (such as S_1 ($n\pi^*$) → $T(\pi\pi^*)$ or S_1 ($\pi\pi^*$) → $T(n\pi^*)$) than the same configuration (such as S_1 ($n\pi^*$) → $T(n\pi^*)$ or $S_1(\pi\pi^*)$ → $T(\pi\pi^*)$). Probable estimates are 10^9-10^8 s^{-1} and 10^6-10^5 s^{-1} for the former and latter cases, respectively. If the rate of ISC is the dominant deactivation process in the $S_{n\pi^*}$ state, the result of a ≪ 30 ns rise time for the triplet-state population suggests a fast $S_{n\pi^*} \rightarrow T_{\pi\pi^*}$ ISC.

4.2. Photophysics in Hydrogen-Bonded Complexes. The ${}^1n \rightarrow \pi^*$ transition normally corresponds to a hypsochromic shift when the corresponding nonbonding valence electrons are directly involved in the HB formation. Such an effect can be rationalized by the stabilization of lone pair electrons upon forming a hydrogen bond. However, for 3FAI/guest HB complexes the dual hydrogen bonding formation mainly incorporates pyrrolic N−H (proton donor) and pyridinal nitrogen (proton acceptor), while the carbonyl oxygen does not play a role in the HB complex formation. Accordingly, it is reasonable to assume that the $S_{n\pi^*}$ configuration remains in the lowest excited singlet state even upon forming 3FAI/guest HB complexes. On the basis of this proposed mechanism we first focus on the dynamics of ESDPT of 3FAI in alcohols. Subsequently, the discussion regarding the relaxation dynamics of 3FAI dimer and 3FAI/guest HB complexes is presented.

3FAI in Alcohols. The dynamics of excited-state proton transfer of 7AI in alcohols have been extensively studied. Using a picosecond transient Kerr-gating technique McMorrow and Aartsma[11] have concluded that the proton-transfer reaction time, depending on various alcohols, is in the range of few hundred picoseconds. Such a time scale is exceedingly slower than the subpicosecond proton-transfer time of the 7AI dimer possessing intact cyclic dual hydrogen bonds.[9,10] The slow reaction rate

SCHEME 1

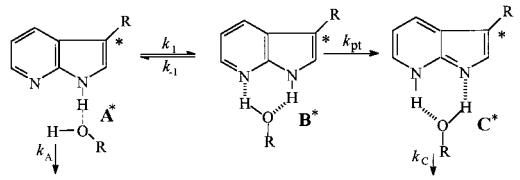

has originally been proposed to be due to the slow solvent reorganization to an appropriate precursor favorable for a relayed type of double proton transfer. The results have been subsequently reconfirmed through more detailed studies based on a time-resolved photon counting technique.[13−15] Consequently, a two-step coupling proton-transfer mechanism has been proposed and depicted in Scheme 1 where * denotes the excited singlet state. The initially predominant species populated in the excited state is ascribed to the A* state which represents a nonspecific HB configuration except for the cyclic dual HB type (i.e., the B* state). The first proton-transfer step incorporates a slow rate of solvent reorganization k_1 to the B* state which possesses a correct geometry for the proton transfer to proceed, coupled with a reverse rate of solvent randomization k_{-1} to any complex formation unfavorable for the proton transfer to proceed. Once in the B* state a competitive rate of intrinsic proton-transfer reaction k_{pt} may take place, forming the tautomer species. Although the solution of the coupling kinetic expression shown in Scheme 1 may not be straightforward, simplification can be made based on the much slower solvent reorganization rate k_1 relative to the k_{-1} and/or k_{pt}. As a result, a steady-state approach can be made for the B* state, and the overall rate of excited-state relaxation dynamics, k_{rxn}, in the A* state can be expressed as

$$k_{rxn} = \frac{k_1 k_{pt} + k_A k_{-1} + k_A k_{pt}}{k_{-1} + k_{pt}} \tag{4}$$

In the case of 7AI k_A is much smaller than k_1, k_{-1} and k_{pt}, Consequently, eq 4 is dominated by the rate of proton-transfer process, which can be further discussed based on two extreme cases. When the intrinsic proton-transfer rate k_{pt} is much faster than k_{-1} (case 1), the overall proton-transfer rate can be expressed as

$$k_{rxn} = k_1 \qquad \text{(case 1)} \tag{5}$$

In this case the overall rate of proton-transfer reaction is mainly determined by the slow solvent reorganization dynamics. Conversely, for case 2 it is assumed that the proton-transfer rate k_{pt} is relatively slower than k_{-1}. Thus, k_{rxn} can be expressed as

$$k_{rxn} = \frac{k_1}{k_{-1}} k_{pt} \qquad \text{(case 2)} \tag{6}$$

In this case, the solvation thermodynamics (i.e., $K_{eq} = k_1/k_{-1}$) coupled with an intrinsic proton transfer rate describe the overall reaction dynamics. Both cases explain the slow solvent-dependent proton-transfer dynamics in various alcohols equally well. However, more detailed isotope, solvent polarity experiments revealed certain discrepancies between two proposed mechanisms.[14,15] More recently, Mentus and Maroncelli[14c] applied a computer simulation on the fractional population of A* and B* states as well as the corresponding molecular dynamics of solvation. The results lead to a conclusion toward the solvation equilibrium controlled mechanism. They further

estimated the intrinsic proton transfer k_{pt} rate to be ca. 0.3 ps^{-1} in methanol, which is on the same order of the magnitude as that obtained experimentally from the 7AI dimer possessing intact dual hydrogen bonds.[9,10] Nevertheless, both mechanisms derived above are in agreement regarding a slower specific solvent reorganization rate which is normally on the order of several hundred picoseconds and is even slower (~1 ns) in water and polyalcohols.

Because of the extremely weak tautomer emission for 3FAI in various alcohols, the possibility of ground-state thermally assisted formation of the double-hydrogen-bonded alcohol complex of 3FAI (such as in structure B of Scheme 1) which, upon direct excitation, gives rise to the tautomer emission has to be considered. However, such a possibility may be discounted by the deuterated 3FAI (3FAI(D)) experiment. In the deuterium isotope experiment we found that the tautomer emission intensity of 3FAI(D) titrated by CH_3OD in cyclohexane is ~40% of the nondeuterated 3FAI. If fast ESDPT takes place through the direct excitation of structure B, Φ_{pt} is expected to be ~1 for both 3FAI and 3FAI(D). Assuming similar tautomer emission efficiency (Φ_c) for 3FAI(D) and 3FAI in cyclohexane (vide infra), the observed tautomer emission yield Φ_{obs} ($=\Phi_{pt}\Phi_c$) is expected to be independent of deuterium substitution. This proposed mechanism contradicts the observed deuterium isotope effect on the tautomer emission intensity. Alternatively, the extremely weak tautomer emission for 3FAI in various alcohols can be rationalized based on the same framework of the above-proposed mechanism (see Scheme 1 and eq 4). However, the rate of nonproton-transfer decay channel (i.e., k_A) in state A* is no longer negligibly slow due to a fast $S_{\pi\pi^*} \rightarrow S_{n\pi^*}$ IC. Thus, the mechanism of ESDPT of 3FAI in alcohols is mainly based on a slower solvent reorganization rate in competition with a much faster $S_{\pi\pi^*} \rightarrow S_{n\pi^*}$ IC. The fraction of proton-transfer process versus the overall relaxation dynamics, Φ_{pt}, is deduced to be either $\Phi_{pt} = k_1/(k_1 + k_A) \sim k_1/k_A$ or $\Phi_{pt} = [(k_1/k_{-1})k_{pt}]/[(k_1/k_{-1})k_{pt} + k_A] \sim [(k_1/k_{-1})k_{pt}]/k_A$, depending on which model, i.e., solvation dynamics or thermodynamics, used to elaborate the ESDPT dynamics in alcohols. For the convenience of the following discussion we simply use a notation k_{pt}' to represent the rate of overall proton-transfer reaction. As a result, Φ_{pt} can be generally expressed as k_{pt}'/k_A in the case of 3FAI in alcohols. The experimentally observed fluorescence yield of the tautomer emission (i.e., C*) can be expressed as $\Phi_{obs} = \Phi_{pt}\Phi_c$ where Φ_c is the fluorescence quantum yield of the tautomer emission under the condition of $\Phi_{pt} = 1$. Although Φ_c was experimentally unobtainable, a reasonable approach can be made by assuming that both 3FAI tautomer and 3FMPP have the same radiative decay rate. The emission yield and decay rate of 3FMPP were measured to be 0.07 and 8.8×10^7 s^{-1}, respectively in methanol (see Table 1), hence a radiative decay rate of 6.2×10^6 s^{-1} was deduced. The tautomer decay rate of 3FAI in methanol was measured to be 1.2×10^8 s^{-1} (see Table 1) we then calculate Φ_c to be 0.052 for 3FAI(tautomer) in methanol. Giving $\Phi_{obs} = \Phi_{pt}\Phi_c$ where Φ_{obs} and Φ_c were 9.5×10^{-5} and 0.052, respectively, a value of Φ_{pt} of $\sim 1.83 \times 10^{-3}$ was then deduced. In another approach, both 7AI and 3FAI possess a similar molecular structure on the proton donating and accepting sites where the dynamics of ESDPT are rate limited by the solvation thermodynamics (or dynamics) in alcohols. Thus, it is reasonable to take the solvent incorporated proton-transfer rate of 8×10^9 s^{-1} (~125 ps[14]) for 7AI in methanol to be the k_{pt}' value for 3FAI in methanol. Since Φ_{pt} can be expressed as k_{pt}'/k_A, a k_A value, i.e., the decay rate attributed to the nonproton-transfer processes, is deduced to be 4.37×10^{12} s^{-1} (~230 fs^{-1}). Such an unusually large k_A value can be reasonably attributed to a fast rate of $S_{\pi\pi^*} \rightarrow S_{n\pi^*}$ IC.

The above kinetic derivation is base on a stance that the proton-transfer reaction is prohibited in the $S_{n\pi^*}$ state for the case of 3FAI HB complexes. Although this happens to be the first case in 7AI analogues, the proposed unfavorable proton transfers in the $S_{n\pi^*}$ state is not uncommon. Cases of the $n\pi^*$ and $\pi\pi^*$ states mixing based on the theoretical approach have been reported in several excited-state intramolecular proton transfer (ESIPT) molecules. For example, the OCCCN ring in 1-amino-3-propenal has been treated as a model for the 2-(2′-hydroxyphenyl) benzothiazole (HBT) and 2-(2′-hydroxyphenyl)-benzoxazole (HBO) which undergo excited-state intramolecular proton transfer (ESIPT) reaction.[35] Ab initio calculations give an $n\pi^*$ and an $\pi\pi^*$ excited states that are nearly isoenergetic for geometry identical to that of the enol ground state. Optimization of geometry in the excited-state results in an enol minimum of the $n\pi^*$ state with a high barrier for proton transfer. As for another example, ab initio calculations of *o*-hydroxybenzaldehyde[36] and *o*-hydroxyacetophenone[37] have predicted no barrier of ESIPT in the first excited $S_{\pi\pi^*}$ state. Whereas the ESIPT in the $S_{n\pi^*}$ state possesses a substantial barrier. For the case of 3FAI, the $^1n\pi^*$ configuration is expected to increase the electron donating ability of the carbonyl oxygen, hence increases the electron density in the pyrrolic system. The consequence may lead to a decrease of the N(1)−H acidity, resulting in the frustration for ESDPT. Further theoretical approaches will be of interest to resolve this issue. The decay dynamics in the $S_{n\pi^*}$ state are thus dominated by intersystem crossing and internal conversion, rationalizing the lack of normal fluorescence for 3FAI in alcohols.

3FAI/Guest Dual HB Complexes. In contrast to the extremely weak or none luminescence behavior of 3FAI in alcohols, the observation of a unique, relatively much stronger tautomer emission among 3FAI dimer, 3FAI/acid and 3FAI/lactam complexes is intriguing. Because of the nearly unaffected carbonyl oxygen in the dual hydrogen bonding formation it is reasonable to conclude that $S_{n\pi^*}$ is also in the lowest excited singlet state for three studied 3FAI HB complexes. As concluded in the absorption and emission titration experiments these three 3FAI HB complexes should possess intact cyclic dual hydrogen bonds. This viewpoint can be supported by a theoretical approach (6-31G(d,p)) in which the calculation based on a dual HB geometry estimates a large formation enthalpy of −10.79, −12.86 and −11.74 kcal/mol for 3FAI dimer, 3FAI/acetic acid and 3FAI/lactam, respectively. Note that for the 7AI dimer possessing intact cyclic dual hydrogen bonds ESDPT takes place with a negligible geometry adjustment, resulting in an ultrafast intrinsic proton-transfer reaction time of ≤1 ps.[9,10] Accordingly, a large-amplitude reorientation of the guest molecule is not necessary upon executing the ESDPT reaction, and hence Scheme 1 can be simplified to Scheme 2 for the three studied HB complexes (only the 3FAI dimer is shown in Scheme 2). In Scheme 2 whether k_{pt} incorporates concerted or sequential process is not known at this stage and is irrelevant to the following discussion. Upon an allowed $\pi-\pi^*$ excitation to the $S_{\pi\pi^*}$ state (the ^1L_a or ^1L_b band, or a state mixing between L_a and L_b) competitive relaxation pathways take place between a fast $S_{\pi\pi^*} \rightarrow S_{n\pi^*}$ IC and an intrinsic rate of proton-transfer reaction, k_{pt}. The fraction for each individual deactivation process can be qualitatively estimated as follows. The observed yields of tautomer emission, Φ_{obs}, for 3FAI dimer, 3FAI/acetic acid and 3FAI/lactam complexes were measured to 0.021, 0.042 and 0.0028, respectively. Similar to that derived in methanol it

SCHEME 2

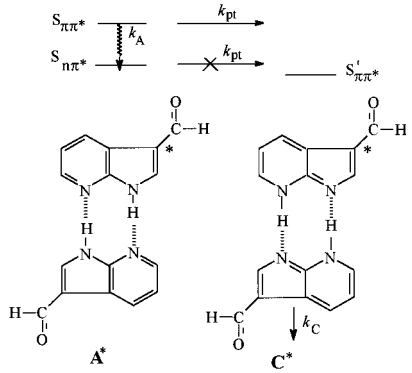

is also reasonable to assume a similar radiative decay rate between 3FMPP and 3FAI(tautomer) HB complexes in cyclohexane. Giving the emission yield and decay rate of 3FMPP to be 0.085 and 8.1×10^7 s^{-1} (see Table 1), a radiative decay rate k_r of 6.9×10^6 s^{-1} was then deduced in cyclohexane. The lifetime of the tautomer emission for each 3FAI/guest complex has been measured and shown in Table 1. Consequently, Φ_c was calculated to be 0.053, 0.077, and 0.054 for 3FAI dimer, 3FAI/acetic acid and 3FAI/lactam, respectively. The relatively smaller Φ_c value with respect to that of 3FMPP can be rationalized by the HB effect in 3FAI(tautomer)/guest complexes, which may induce additional radiationless decay channels. On the basis of the relation of $\Phi_{pt} = \Phi_{obs}/\Phi_c$, Φ_{pt} was then calculated to be 0.40 and 0.55 for 3FAI dimer and 3FAI/acetic acid complex, respectively. Φ_{pt} can be further expressed as $\Phi_{pt} = k_{pt}/(k_{pt} + k_A)$ according to Scheme 2. Since the rate of $S_{n\pi^*} \rightarrow S_{\pi\pi^*}$ IC is commonly independent of solvents it is reasonable to adopt same k_A (IC) rate of 4.37×10^{12} s^{-1} estimated in methanol for three studied 3FAI HB complexes. Accordingly, an intrinsic proton-transfer rate k_{pt} of 2.91×10^{12} s^{-1} (343 fs^{-1}) and 5.34×10^{12} s^{-1} (187 fs^{-1}) was deduced for 3FAI dimer and 3FAI/acetic acid complex, respectively. These values are qualitatively in agreement with the rate of proton transfer of $\geq 1.0 \times 10^{12}$ s^{-1} reported in the case of 7AI dimer.[9,10] Assuming similar rate of IC and Φ_c upon the N−H deuterium substitution, the deuterium isotope-dependent tautomer emission intensity can thus be rationalized by the slower deuterium transfer rate relative that of proton. As a result, k_{pt} for deuterium transfer is less competitive with respect to the rate of IC. For example, giving Φ_{obs} of 0.03 (vide supra) for the 3FAI(D)/acetic acid(D) complex, k^D_{pt} was then estimated to be ~ 360 fs^{-1}. Similar method gives a k^D_{pt} value of 675 fs^{-1} for the 3FAI(D) dimer. Note that in this study negligible deuterium isotope effect was observed in the steady-state tautomer emission intensity for the 7AI dimer where k_{pt} is apparently $\gg k_A$, although significant deuterium transfer dynamics have been reported.[10]

Interestingly, Φ_{obs} for the 3FAI/lactam complex is only ca. 6.7% of that measured in 3FAI/acetic acid (see Table 1). If the assumption of a similar Φ_c holds among three studied 3FAI HB complexes, a smaller k_{pt} value of 2.4×10^{11} s^{-1} (4.2 ps^{-1}) was then estimated for the 3FAI/lactam HB complex. The ESDPT reaction in 3FAI/lactam can be ascribed as a noncatalytic type[16c,d] where both host and guest should undergo tautomerism simultaneously during ESDPT. The more endergonic reaction may empirically lead to a higher formation free energy of the activated complex, i.e., an existence of higher energy barrier. Further investigation focusing on the ultrafast time-resolved ESDPT dynamics is necessary to resolve this issue.

For all studied 3FAI HB species appreciable population in the normal triplet state is expected. Accordingly, a key question regarding the double proton transfer in the triplet state, i.e., T → T′ (prime denotes the tautomer species) is intriguing. We have attempted to perform the triplet−triplet absorption measurement in the concentrated 3FAI. Unfortunately, since the spectral profiles remain unchanged during the time-dependent spectral evolution this issue cannot be resolved at this stage. On one hand, the result may indicate the prohibition of the T → T′ proton transfer reaction. On the other hand, it might indicate that ESDPT in the triplet state takes place at a time scale much shorter than the system response time of 30 ns so that the observed transient spectra mainly correspond to the $T_1' \rightarrow T_n'$ transition. Further studies focusing on the dynamics of proton transfer reaction in the triplet state for 3FAI HB complexes are currently in progress.

Conclusion

In summary the $^1n\pi^*$ configuration is concluded to be in the lowest excited singlet state for both normal monomer and HB complexes in 3FAI. An $S_{\pi\pi^*} \rightarrow S_{n\pi^*}$ IC rate has been estimated to be ~ 230 fs^{-1} in methanol. ESDPT of 3FAI in alcohols, similar to that of the 7AI/alcohols complex, requires a geometrical adjustment of the guest molecule on a time scale of few hundred picoseconds and thus can hardly compete with the $S_{\pi\pi^*} \rightarrow S_{n\pi^*}$ IC. On the other hand, the intact dual HB formation in the cases of 3FAI dimer, 3FAI/acetic acid and 3FAI/lactam complexes leads to a fast ESDPT which is comparable with the rate of $S_{\pi\pi^*} \rightarrow S_{n\pi^*}$ IC. Accordingly, the steady-state tautomer emission intensity reveals a remarkable deuterium isotope effect. The introduction of a carbonyl functional group at the C_3 position thus presents the first case among 7AI analogues to demonstrate the competitive IC/ESDPT reaction in which the fast $S_{\pi\pi^*} \rightarrow S_{n\pi^*}$ IC serves as an internal clock to examine the dynamics of ESDPT.

Acknowledgment. This work was supported by the National Science Council, Taiwan, R.O.C. (NSC87-2119-M-194-002).

References and Notes

(1) Taylor, C. A.; El-Bayoumi, A. M.; Kasha, M. *Proc. Natl. Acad. Sci. U.S.A.* **1969,** *65*, 253

(2) Ingham, K. C.; El-Bayoumi, M. A. *J. Am. Chem. Soc.* **1971**, *93*, 5023.

(3) Ingham. K. C.; El-Bayoumi, M. A. *J. Am. Chem. Soc.* **1974**, *96*, 1674.

(4) Watson, J. D.; Crick, F. H. C. *Nature (London)* **1953**, *171*, 964.

(5) Watson, D. G.; Sweet, R. M.; Marsh, R. E. *Acta Crystallogr.* **1965**, *19*, 573.

(6) Douhal, A.; Kim, S. K.; Zewail, A. H. *Nature* **1995**, *378*.

(7) Folmer, D. E.; Poth, L.; Wisniewski, E. S.; Castleman, A. W., Jr. *Chem. Phys. Lett.* **1998**, *287*, 1.

(8) Chachisvillis, M.; Fiebig, T.; Douhal, A.; Zewail, A. H. *J. Phys. Chem. A.* **1998**, *102*, 669.

(9) Takeuchi, S.; Tahara, T. *J. Phys. Chem. A* **1998**, *102*, 7740.

(10) Fiebig, T.; Chachisvillis, M.; Manger, M.; Zewail, A. H.; Douhal, A.; Garcia Ochoa, I.; de La Hoz Ayuso, A.*J. Phys. Chem. A* **1999**, *103*, 7419.

(11) McMorrow, D.; Aartsma, T. *Chem. Phys. Lett.* **1986**, *125*, 581.

(12) Moog, R. S.; Bovino, S. C.; Simon, J. D. *J. Phys. Chem.* **1988,** *92*, 6545.

(13) Koijnenberg, J.; Huizer, A. H.; Varma, C. A. O. *J. Chem. Soc., Faraday Trans. 2* **1988**, *84* (8), 1163.

(14) (a) Moog., R. S.; Maroncelli, M. *J. Phys. Chem.* **1991**, *95*, 10359. (b) Chapman, C. F.; Maroncelli, M. *J. Phys. Chem.* **1992**, *96*, 8430. (c) Mentus, S.; Maroncelli, M. *J. Phys. Chem. A* **1998**, *102*, 3860.

(15) (a) Negreie, M.; Bellefeuille, S. M.; Whitham, S.; Petrich, J. W.; Thornburg, R. W. *J. Am. Chem. Soc.* **1990**, *112*, 7419. (b) Negrerie, M.; Gai, F.; Bellefeuille, S. M.; Petrich, J. W. *J. Phys. Chem.* **1991,** *95*, 8663. (c) Negrerie, M.; Gai, F.; Lambry, J.-C.; Martin, J.-L.; Petrich, J. W. *J. Phys. Chem.* **1993,** *97*, 5046. (d) Chen, Y.; Rich, R. L.; Gai, F.; Petrich, J.

W. *J. Phys. Chem*. **1993**, *97*, 1770. (e) Chen, Y.; Gai, F.; Petrich, J. W. *J. Am. Chem. Soc.* **1993**, *115*, 10158. (f) Rich, R. L.; Chen, Y.; Neven, D.; Negrerie, M.; Gai, F.; Petrich, J. W. *J. Phys. Chem.* **1993**, *97*, 1781. (g) Gai, F.; Rich, R. L.; Petrich, J. W. *J. Am. Chem. Soc.* **1994**, *116*, 735. (h) Smirnov, A. V.; English, D. S.; Rich, R. L.; Lane, J. Teyton, L.; Schwabacher, A. W.; Luo, S.; Thornburg, R. W.; Petrich, J. W. *J. Phys. Chem.* **1997**, *101B*, 2758 and references therein.

(16) (a) Chou, P. T.; Martinez, M. L.; Cooper, W. C.; McMorrow, D.; Collin, S. T.; Kasha; M. *J. Phys. Chem.* **1992**, *96*, 5203. (b) Chang, C. P.; Hwang, W. C.; Kuo M. S.; Chou, P. T.; Clement, J. H. *J. Phys. Chem.* **1994**, *98*, 8801. (c) Chou, P. T.; Wei, C. Y.; Chang, C. P.; Chiu, C. H. *J. Am. Chem. Soc.* **1995**, *117*, 7259. (d) Chou, P. T.; Wei, C. Y.; Chang, C. P.; Kuo, M. S. *J. Phys. Chem.* **1995**, *99*, 11994. (e) Chou, P. T.; Yu, W. S.; Chen, Y. C.; Wei, C. Y.; Martinez, S. S. *J. Am. Chem. Soc.* **1998**, *120*, 12927.

(17) Chaban, G. M.; Gordan, M. S. *J. Phys. Chem. A* **1999**, *103*, 185.

(18) Chou, P. T.; Wei, C. Y.; Wu, G. R.; Chen, W. S. *J. Am. Chem. Soc.* **1999**, *121*, 12186.

(19) Chou, P. T.; Wu, G. R.; Wei, C. Y.; Cheng, C. C.; Chang, C. P.; Hung, F. T. *J. Phys. Chem. B* **1999**, *103*, 10042.

(20) Robsion, M. M.; Robison, B. L. *J. Am. Chem. Soc.* **1955**, *77*, 457.

(21) Demas, J. N.; Crosby, G. A. *J. Phys. Chem.* **1971**, *75*, 991−1024.

(22) Olness, D.; Sponer, H. *J. Chem. Phys.* **1963**, *38*, 1799.

(23) Chou, P. T.; Wei, C. Y.; Hung, F. T. *J. Phys. Chem. B* **1997**, *101*, 9119.

(24) Foresman, J. B.; Head-Gordon, M.; Pople, J. A.; Frisch, M. J. *J. Phys. Chem.* **1992**, *96*, 135.

(25) Petersson, G. A.; Malick, D. K.; Wilson, W. G.; Ochterski, J. W.; Montgomery, J. A, Jr.; Frisch, M. J. *J. Chem. Phys*. **1998**, *109*, 10570.

(26) Bauernschmitt, R.; Ahlrichs, R. *Chem. Phys. Lett.* **1996**, *256*, 454.

(27) Casida, M. E.; Jamorski, C.; Casida, K. C.; Salahub, D. R. *J. Chem. Phys*. **1998**, *108*, 4439.

(28) Platt, J. R. *J. Chem. Phys.* **1949**, *17*, 484.

(29) Valeur, B.; Weber, G. *Photochem. Photobiol.* **1977**, *25*, 441.

(30) Ilich, P. *J. Mol. Struct.* **1995**, *354*, 37.

(31) Note that the L_a band has been reported to be in the lowest excited singlet state upon forming HB complexes such as the 7AI dimer.[9]

(32) Appreciable amount of the singlet oxygen ($^1\Delta_g \rightarrow {}^3\Sigma^-_g(0,0)$) 1273 nm emission sensitized by 3FAI was detected. A detailed description of the near-IR detecting system has been given in ref 33.

(33) Chou; P. T.; Chen, Y. C.; Wei, C. Y.; Chen, S. J.; Lu, H. L. *J. Phys. Chem. A* **1997**, *101*, 8581.

(34) El-Sayed, M. A. *J. Chem. Phys.* **1963**, *38*, 2834.

(35) Sobolewski, A. L.; Domcke, W. *Chem. Phys. Lett.* **1993**, *211*, 82.

(36) Sobolewski, A. L.; Domcke, W. *Chem. Phys.* **1994**, *184*, 115.

(37) Vener, M. V.; Scheiner, S. *J. Phys. Chem.* **1995**, *99*, 642.